

# Vibration Suppression and Optimal Repetitive Disturbance Rejection Control in Semi-Nyquist Frequency Region using Multirate Sampling Control

Hiroshi Fujimoto and Yoichi Hori

Department of Electrical Engineering, The University of Tokyo

7-3-1 Hongo, Bunkyo, Tokyo, 113-8656, Japan

E-mail: fuji@hori.t.u-tokyo.ac.jp, hori@hori.t.u-tokyo.ac.jp

## Abstract

In this paper, novel multirate feedback controllers are proposed for digital control systems with relatively long sampling period. The proposed controllers achieve vibration suppression and disturbance rejection even in the semi-Nyquist frequency region. First, the continuous-time vibration suppression controller is exactly discretized by the multirate sampling control based on the closed-loop characteristics. Second, the multirate repetitive controllers are proposed both by the feedback and feedforward approaches. Moreover, the inter-sample disturbance rejection performance is optimized by the fast sampling approach. The proposed controllers are applied to the settling and following modes of hard disk drive, and the advantages of these approaches are demonstrated by simulations.

## 1 Introduction

A digital control system generally has a sampler for the plant output  $y(t)$ , and one holder of the control input  $u(t)$ . The sampling period of the output  $T_y$  is generally decided by the speed of the sensor or the A/D converter. On the other hand, the control period of the input  $T_u$  is also determined by the speed of the actuator, D/A converter, or the calculation on the CPU. In practical control systems, these periods are usually restricted by the hardware. In this paper, the digital control systems with longer sampling period ( $T_u < T_y$ ) are considered. This restriction may be general because D/A converters are usually faster than the A/D converters. Especially, head-positioning systems of the hard disk drive (HDD) or the visual servo systems of robot manipulator belong to this category, because the sampling rates of the measurement are relatively slow [1]–[3].

For these systems, it is difficult to suppress vibration and to reject disturbance in high frequency region because the Nyquist frequency is relatively low. In this paper, multirate sampling control is introduced, in which the plant input is changed  $N$  times during one sampling period. This scheme is also called the multirate input control. Using this scheme, novel multirate feedback controllers are proposed, which achieve vibration suppression and disturbance rejection even in the

semi-Nyquist frequency region. Moreover, the proposed methods are applied to the head-positioning system of hard disk drive.

Vibration suppression controllers have been proposed by the various approaches in the continuous-time system. To implement them in the digital control systems, the designed analog controllers are discretized by the Tustin transformation or other methods. Because these transformations are based only on the open-loop characteristics of the controller, the closed-loop becomes low performance or unstable when the resonance mode is close to the Nyquist frequency.

On the other hand, introducing multirate sampling control, the authors proposed a novel discretization method of controllers based on the closed-loop characteristics [4]. In this paper, this approach is extended to the hardware restriction of ( $T_u < T_y$ ) and applied to the vibration suppression controller. The advantages of the proposed method are that the controller is discretized based on the closed-loop characteristics, and the plant state of the digitally controlled system completely matches that of the original continuous-time system at  $M$  inter-sample points during  $T_y$ .

In the repetitive control system [5], conventional single-rate controllers do not have enough inter-sample performance to reject disturbance in the semi-Nyquist frequency region [6]. On the other hand, authors proposed a novel multirate feedback controller, which achieves the perfect disturbance rejection at  $M$  inter-sample points [3]. In this paper, the proposed approach is modified to repetitive control, and applied to reject high order repeatable run-out of hard disk drive.

Repetitive feedback controllers based on the internal model principle have disadvantages that the closed-loop characteristics become worse and difficult to assure stability robustness [6]. Therefore, this paper proposes novel approach that never has these problems, based on the open-loop estimation and disturbance rejection by feedforward approach.

## 2 Discretization of controller based on multirate control

In this section, novel discretization method of an analog controller is proposed for the system with longer

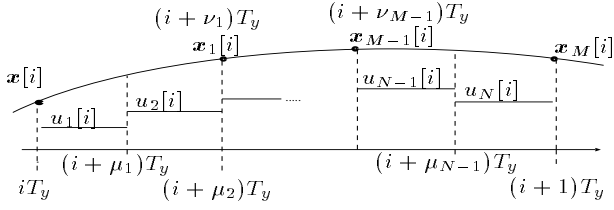


**Figure 1:** Multirate sampling control.

sampling period ( $T_u < T_y$ ) base on the multirate input control. The proposed method is applied to vibration suppression controller in section 4.1. In the proposed multirate scheme, the plant input is changed  $N$  times during  $T_y$  and the plant state is evaluated  $M$  times in this interval as shown in Fig. 1. The positive integers  $M$  and  $N$  are referred to as input and state multiplicities, respectively.  $N$  is determined by the hardware restriction. In this paper, the state multiplicity is defined as  $M = N/n$  except for section 3.3, where  $n$  is the plant order.

In Fig. 1,  $\mu_j (j = 0, 1, \dots, N)$  and  $\nu_k (k = 1, \dots, M)$  are the parameters for the timing of the input changing and the state evaluation, which satisfy the conditions (1) and (2).

$$0 = \mu_0 < \mu_1 < \mu_2 < \dots < \mu_N = 1 \quad (1)$$

$$0 < \nu_1 < \nu_2 < \dots < \nu_M = 1 \quad (2)$$

If  $T_y$  is divided at same intervals, the parameters are set to  $\mu_j = j/N, \nu_k = k/M$ .

For simplification, the continuous-time plant is assumed to be SISO system in this paper. The proposed methods, however, can be extended to deal with the MIMO system by the same way as [4].

## 2.1 Plant Discretization by Multirate Sampling

Consider the continuous-time plant described by

$$\dot{\mathbf{x}}(t) = \mathbf{A}_c \mathbf{x}(t) + \mathbf{b}_c u(t), \quad y(t) = \mathbf{c}_c \mathbf{x}(t). \quad (3)$$

The discrete-time plant discretized by the multirate sampling control (Fig. 1) becomes

$$\mathbf{x}[i+1] = \mathbf{A} \mathbf{x}[i] + \mathbf{B} \mathbf{u}[i], \quad y[i] = \mathbf{C} \mathbf{x}[i], \quad (4)$$

where  $\mathbf{x}[i] = \mathbf{x}(iT)$ , and matrices  $\mathbf{A}, \mathbf{B}, \mathbf{C}$  and vectors  $\mathbf{u}$  are given by

$$\begin{bmatrix} \mathbf{A} & \mathbf{B} \\ \mathbf{C} & \mathbf{O} \end{bmatrix} := \begin{bmatrix} e^{\mathbf{A}_c T_y} & \mathbf{b}_1 & \dots & \mathbf{b}_N \\ \mathbf{c}_c & 0 & \dots & 0 \end{bmatrix}, \quad (5)$$

$$\mathbf{b}_j := \int_{(1-\mu_j)T_y}^{(1-\mu_{(j-1)})T_y} e^{\mathbf{A}_c \tau} \mathbf{b}_c d\tau, \quad \mathbf{u} := [u_1, \dots, u_N]^T, \quad (6)$$

The inter-sample plant state at  $t = (i + \nu_k)T_y$  is represented by

$$\tilde{\mathbf{x}}[i] = \tilde{\mathbf{A}} \mathbf{x}[i] + \tilde{\mathbf{B}} \mathbf{u}[i], \quad (7)$$

$$\begin{bmatrix} \tilde{\mathbf{A}} & \tilde{\mathbf{B}} \end{bmatrix} := \begin{bmatrix} \tilde{\mathbf{A}}_1 & \tilde{\mathbf{b}}_{11} & \dots & \tilde{\mathbf{b}}_{1N} \\ \vdots & \vdots & & \vdots \\ \tilde{\mathbf{A}}_M & \tilde{\mathbf{b}}_{M1} & \dots & \tilde{\mathbf{b}}_{MN} \end{bmatrix}, \quad (8)$$

$$\tilde{\mathbf{A}}_k := e^{\mathbf{A}_c \nu_k T_y}, \quad \tilde{\mathbf{x}} := [\mathbf{x}_1, \dots, \mathbf{x}_M]^T, \quad (9)$$

$$\mathbf{x}_k[i] = \mathbf{x}[i + \nu_k] = \mathbf{x}((i + \nu_k)T_y), \quad (10)$$

$$\tilde{\mathbf{b}}_{kj} := \begin{cases} \mu_j < \nu_k : & \int_{(\nu_k - \mu_{(j-1)})T_y}^{(\nu_k - \mu_j)T_y} e^{\mathbf{A}_c \tau} \mathbf{b}_c d\tau \\ \mu_{(j-1)} < \nu_k \leq \mu_j : & \int_0^{(\nu_k - \mu_{(j-1)})T_y} e^{\mathbf{A}_c \tau} \mathbf{b}_c d\tau \\ \nu_k \leq \mu_{(j-1)} : & 0 \end{cases},$$

## 2.2 Design of continuous-time controller

In this section, the continuous-time controller is designed based on the regulator and the disturbance observer. Consider the continuous-time plant model described by

$$\dot{\mathbf{x}}_p(t) = \mathbf{A}_{cp} \mathbf{x}_p(t) + \mathbf{b}_{cp}(u(t) - d(t)) \quad (11)$$

$$y(t) = \mathbf{c}_{cp} \mathbf{x}_p(t), \quad (12)$$

where  $d(t)$  is the disturbance input. Let the disturbance model be

$$\dot{\mathbf{x}}_d(t) = \mathbf{A}_{cd} \mathbf{x}_d(t), \quad d(t) = \mathbf{c}_{cd} \mathbf{x}_d(t). \quad (13)$$

For example, the sinusoidal type disturbance with frequency  $\omega_d$  is modeled by

$$\mathbf{A}_{cd} = \begin{bmatrix} 0 & 1 \\ -\omega_d^2 & 0 \end{bmatrix}, \quad \mathbf{c}_{cd} = [1, 0]. \quad (14)$$

The continuous-time augmented system consisting of (11) and (13) is represented by

$$\dot{\mathbf{x}}(t) = \mathbf{A}_c \mathbf{x}(t) + \mathbf{b}_c u(t), \quad y(t) = \mathbf{c}_c \mathbf{x}(t), \quad (15)$$

$$\mathbf{A}_c := \begin{bmatrix} \mathbf{A}_{cp} & -\mathbf{b}_{cp} \mathbf{c}_{cd} \\ \mathbf{O} & \mathbf{A}_{cd} \end{bmatrix}, \quad \mathbf{b}_c := \begin{bmatrix} \mathbf{b}_{cp} \\ \mathbf{O} \end{bmatrix}, \quad \mathbf{x} := \begin{bmatrix} \mathbf{x}_p \\ \mathbf{x}_d \end{bmatrix},$$

where  $\mathbf{c}_c := [\mathbf{c}_{cp}, \mathbf{O}]$ . For the plant (15), the continuous-time observer is designed from the Gopinath's method by

$$\dot{\hat{\mathbf{v}}}(t) = \hat{\mathbf{A}}_c \hat{\mathbf{v}}(t) + \hat{\mathbf{b}}_c y(t) + \hat{\mathbf{J}}_c u(t) \quad (16)$$

$$\hat{\mathbf{x}}(t) = \hat{\mathbf{C}}_c \hat{\mathbf{v}}(t) + \hat{\mathbf{d}}_c y(t). \quad (17)$$

In order to regulate the plant state and reject the disturbance, the continuous-time regulator is designed by

$$u(t) = \mathbf{f}_{cp} \hat{\mathbf{x}}_p(t) + \mathbf{c}_{cd} \hat{\mathbf{x}}_d(t) = \mathbf{f}_c \hat{\mathbf{x}}(t), \quad (18)$$

where  $\mathbf{f}_c := [\mathbf{f}_{cp}, \mathbf{c}_{cd}]$ . Letting  $\mathbf{e}_v$  be the estimation errors of the observer ( $\mathbf{e}_v = \hat{\mathbf{v}} - \mathbf{v}$ ), the following equation is obtained.

$$\dot{\hat{\mathbf{x}}}(t) = \mathbf{x}(t) + \hat{\mathbf{C}} \mathbf{e}_v(t). \quad (19)$$

From the above equations, the closed-loop system is represented by

$$\begin{bmatrix} \dot{\mathbf{x}}_p(t) \\ \dot{\mathbf{x}}_d(t) \\ \dot{\mathbf{e}}_v(t) \end{bmatrix} = \begin{bmatrix} \mathbf{A}_f & \mathbf{O} & \mathbf{b}_{cp} \mathbf{f}_c \hat{\mathbf{C}}_c \\ \mathbf{O} & \mathbf{A}_d & \mathbf{O} \\ \mathbf{O} & \mathbf{O} & \hat{\mathbf{A}}_c \end{bmatrix} \begin{bmatrix} \mathbf{x}_p(t) \\ \mathbf{x}_d(t) \\ \mathbf{e}_v(t) \end{bmatrix}, \quad (20)$$

where  $\mathbf{A}_f := \mathbf{A}_{cp} + \mathbf{b}_{cp} \mathbf{f}_{cp}$ . The transitions of the states  $\mathbf{x}_p, \mathbf{x}_d$  from  $t = iT_y$  to  $t = (i + \nu_k)T_y$  are represented by

$$\begin{bmatrix} \mathbf{x}_p[i + \nu_k] \\ \mathbf{x}_d[i + \nu_k] \\ \mathbf{e}_v[i + 1] \end{bmatrix} = \begin{bmatrix} e^{\mathbf{A}_f \nu_k T_y} & \mathbf{O} & * \\ \mathbf{O} & e^{\mathbf{A}_d \nu_k T_y} & \mathbf{O} \\ \mathbf{O} & \mathbf{O} & e^{\hat{\mathbf{A}}_c T_y} \end{bmatrix} \begin{bmatrix} \mathbf{x}_p[i] \\ \mathbf{x}_d[i] \\ \mathbf{e}_v[i] \end{bmatrix}. \quad (21)$$

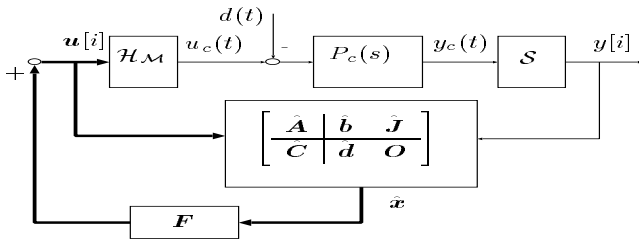


Figure 2: Multirate control with disturbance observer.

### 2.3 Discretization of the controller by multirate control

In this section, the digital controller is obtained from the continuous-time controller designed in section 2.2 using multirate input control. Discretizing (15) by the multirate sampling control, the inter-sample plant state at  $t = (i + \nu_k)T_y$  can be calculated from the  $k$ th row of (7) by

$$\mathbf{x}[i + \nu_k] = \tilde{\mathbf{A}}_k \mathbf{x}[i] + \tilde{\mathbf{B}}_k \mathbf{u}[i] \quad (22)$$

$$\tilde{\mathbf{A}}_k = \begin{bmatrix} \tilde{\mathbf{A}}_{pk} & \tilde{\mathbf{A}}_{pdk} \\ \mathbf{O} & \tilde{\mathbf{A}}_{dk} \end{bmatrix}, \tilde{\mathbf{B}}_k = \begin{bmatrix} \tilde{\mathbf{B}}_{pk} \\ \mathbf{O} \end{bmatrix}.$$

For the plant (15) discretized by (4), the discrete-time observer on the sampling points is obtained by

$$\hat{\mathbf{v}}[i + 1] = \hat{\mathbf{A}}\hat{\mathbf{v}}[i] + \hat{\mathbf{b}}y[i] + \hat{\mathbf{J}}\mathbf{u}[i] \quad (23)$$

$$\hat{\mathbf{x}}[i] = \hat{\mathbf{C}}\hat{\mathbf{v}}[i] + \hat{\mathbf{d}}y[i]. \quad (24)$$

As shown in Fig. 2, let the feedback control law be

$$\mathbf{u}[i] = \mathbf{F}_p \hat{\mathbf{x}}_p[i] + \mathbf{F}_d \hat{\mathbf{x}}_d[i] = \mathbf{F} \hat{\mathbf{x}}[i], \quad (25)$$

where  $\mathbf{F} := [\mathbf{F}_p, \mathbf{F}_d]$ . From (22) to (25), the closed-loop system is represented by

$$\begin{bmatrix} \mathbf{x}_p[i + \nu_k] \\ \mathbf{x}_d[i + \nu_k] \\ \mathbf{e}_v[i + 1] \end{bmatrix} = \begin{bmatrix} \tilde{\mathbf{A}}_{pk} + \tilde{\mathbf{B}}_{pk}\mathbf{F}_p & \tilde{\mathbf{A}}_{pdk} + \tilde{\mathbf{B}}_{pk}\mathbf{F}_d & \tilde{\mathbf{B}}_{pk}\mathbf{F}\hat{\mathbf{C}} \\ \mathbf{O} & \tilde{\mathbf{A}}_{dk} & \mathbf{O} \\ \mathbf{O} & \mathbf{O} & \hat{\mathbf{A}} \end{bmatrix} \begin{bmatrix} \mathbf{x}_p[i] \\ \mathbf{x}_d[i] \\ \mathbf{e}_v[i] \end{bmatrix}. \quad (26)$$

Comparing (21) and (26), if the following conditions are satisfied, the plant state ( $\mathbf{x}_p$ ) of the digitally controlled system completely matches that of the original continuous-time system at  $M$  inter-sample points on  $t = (i + \nu_k)T_y$ .

$$\tilde{\mathbf{A}}_{pk} + \tilde{\mathbf{B}}_{pk}\mathbf{F}_p = e^{\mathbf{A}_f \nu_k T_y}, \quad (27)$$

$$\tilde{\mathbf{A}}_{pdk} + \tilde{\mathbf{B}}_{pk}\mathbf{F}_d = \mathbf{O}, \quad (28)$$

$$\mathbf{e}_v[i] = \mathbf{O}. \quad (29)$$

The simultaneous equations of (27) and (28) for all  $k = (1, \dots, M)$  become

$$\tilde{\mathbf{A}}_p + \tilde{\mathbf{B}}_p \mathbf{F}_p = \mathbf{E}, \quad \tilde{\mathbf{A}}_{pd} + \tilde{\mathbf{B}}_p \mathbf{F}_d = \mathbf{O}, \quad (30)$$

where  $\tilde{\mathbf{A}}_p, \tilde{\mathbf{A}}_{pd}, \tilde{\mathbf{B}}_p$  and  $\mathbf{E}$  are defined by

$$\begin{bmatrix} \tilde{\mathbf{A}}_{p1} \\ \vdots \\ \tilde{\mathbf{A}}_{pM} \end{bmatrix}, \begin{bmatrix} \tilde{\mathbf{A}}_{pd1} \\ \vdots \\ \tilde{\mathbf{A}}_{pdM} \end{bmatrix}, \begin{bmatrix} \tilde{\mathbf{B}}_{p1} \\ \vdots \\ \tilde{\mathbf{B}}_{pM} \end{bmatrix}, \begin{bmatrix} e^{\mathbf{A}_f \nu_1 T_y} \\ \vdots \\ e^{\mathbf{A}_f \nu_M T_y} \end{bmatrix}.$$

Because non-singularity of the matrix  $\tilde{\mathbf{B}}_p$  can be assured on  $M = N/n$  [3, 7],  $\mathbf{F}_p$  and  $\mathbf{F}_d$  are obtained by

$$\mathbf{F}_p = \tilde{\mathbf{B}}_p^{-1}(\mathbf{E} - \tilde{\mathbf{A}}_p), \quad \mathbf{F}_d = -\tilde{\mathbf{B}}_p^{-1} \tilde{\mathbf{A}}_{pd}. \quad (31)$$

Moreover, [4] proposed the discretization for observer based on multirate output control, where the plant output is detected more frequently than the control period ( $T_y < T_u$ ). However, in this paper, discrete-time observer (23) is simply obtained, so that the eigenvalues of  $\hat{\mathbf{A}}$  become identical to those of  $\exp(\hat{\mathbf{A}}_c T_y)$ , because the plant is assumed to have longer sampling period ( $T_y > T_u$ ). Substituting (23) for (25), the feedback type controller is obtained by

$$\begin{bmatrix} \hat{\mathbf{v}}[i + 1] \\ \mathbf{u}[i] \end{bmatrix} = \begin{bmatrix} \hat{\mathbf{A}} + \hat{\mathbf{J}}\mathbf{F}\hat{\mathbf{C}} & \hat{\mathbf{b}} + \hat{\mathbf{J}}\mathbf{F}\hat{\mathbf{d}} \\ \mathbf{F}\hat{\mathbf{C}} & \mathbf{F}\hat{\mathbf{d}} \end{bmatrix} \begin{bmatrix} \hat{\mathbf{v}}[i] \\ y[i] \end{bmatrix}. \quad (32)$$

### 2.4 Initial value compensation

In this section, the initial value of the controller (32) is considered in order to eliminate the estimation error of the observer and satisfy (29). From (24), if  $\mathbf{x}[0]$  is known, the initial value of controller should be set by

$$\hat{\mathbf{C}}\hat{\mathbf{v}}[0] = \mathbf{x}[0] - \hat{\mathbf{d}}y[0]. \quad (33)$$

By this compensation, it is possible to prevent the overshoot of the step (or initial value) response because the plant state converges only by the mode of the regulator. Therefore,  $\mathbf{f}_{cp}$  should be designed to assign the eigenvalues of  $\mathbf{A}_f$  to the small (or zero) overshoot region.

### 3 Repetitive control based on multirate control

In this section, two multirate repetitive controllers are proposed, which are 1) feedback approach based on internal model principle and 2) feedforward disturbance rejection approach based on the open-loop estimation.

#### 3.1 Feedback repetitive control

The periodic disturbance of  $T_0 := 2\pi/\omega_0$  is represented by

$$d(t) = a_0 + \sum_{k=1}^{\infty} a_k \cos k\omega_0 t + b_k \sin k\omega_0 t, \quad (34)$$

where  $\omega_0$  is known and  $a_k, b_k$  are unknown parameters. Letting the disturbance model (13) be (34), the repetitive feedback controller is obtained by (32), which has internal model  $s^2 + (k\omega_0)^2$  in discrete-time domain.

From (26) and (28), the influence from disturbance  $\mathbf{x}_d[i]$  to the inter-sample state  $\mathbf{x}_p[i + \nu_k]$  becomes zero

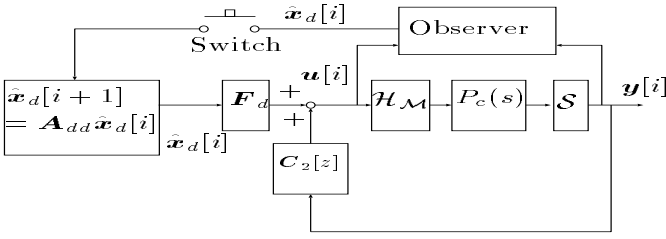


**Figure 3:** Feedforward repetitive control.

at  $t = (i + \nu_k)T_y$ . Moreover,  $\mathbf{x}_p[i]$  and  $\mathbf{e}_v[i]$  converge to zero at the rate of the eigenvalues of  $\tilde{\mathbf{A}}_{pM} + \tilde{\mathbf{B}}_{pM}\mathbf{F}_p$  and  $\hat{\mathbf{A}}$  (the poles of the regulator and observer). Therefore, the repetitive disturbance is perfectly rejected ( $\mathbf{x}_p[i + \nu_k] = 0$ ) at  $M$  inter-sample points in the steady state.

### 3.2 Feedforward repetitive control

The repetitive feedback control based on the internal model principle has disadvantages that the closed-loop characteristics become worse and difficult to assure stability robustness [6]. Therefore, in this section, novel repetitive controller based on the open-loop estimation and feedforward disturbance rejection are proposed as shown in Fig. 3

The repetitive disturbance is estimated by the open-loop disturbance observer. When the estimation converges to the steady state, the switch turns on at  $t = t_0$ . After that, the switch turns off immediately. The repetitive disturbance is calculated by (35) from the initial value  $\hat{\mathbf{x}}_d[t_0]$  which has the amplitude and phase information of the disturbance.

$$\hat{\mathbf{x}}_d[i + 1] = \mathbf{A}_{dd}\hat{\mathbf{x}}_d[i], \quad (35)$$

where  $\mathbf{A}_{dd} = e^{\mathbf{A}_{cd}T_y}$ . Because the disturbance feedforward  $\mathbf{F}_d$  is obtained by (31), the perfect disturbance rejection is achieved at  $M$  inter-sample points. The advantage of this approach is that the stability robustness can be guaranteed easily only by the conventional feedback controller  $\mathbf{C}_2[z]$ .

Moreover, by introducing the initial value compensation of the feedback controller  $\mathbf{C}_2[z]$  at  $t = t_0$ , the transient response can be improved after this switching action. It is possible to prevent the overshoot by setting the initial state  $\hat{\mathbf{v}}[t_0]$  to be (33) using the estimated value of open-loop observer  $\hat{\mathbf{x}}[t_0]$ .

### 3.3 Optimization of the inter-sample disturbance rejection performance

In section 3.1 and section 3.2, the state multiplicity is defined as  $M = N/n$  in order to reject the disturbance perfectly at  $M$  inter-sample points. In this section,  $M$  is selected more than  $N/n$  to optimize the inter-sample performance. This approach is referred to as the fast sampling technique in the modern sampled-data control theory [8, 9, 10].

When  $M$  is selected more than  $N/n$ , it is impossible to satisfy (30) because the number of row of  $\tilde{\mathbf{B}}_p$  is

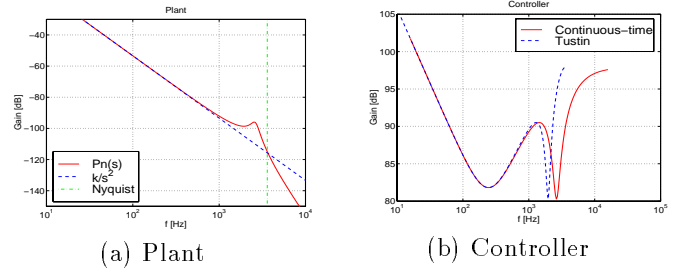


**Figure 4:** Frequency responses.

larger than that of column. Therefore, the inter-sample performance can be optimized by minimizing  $\tilde{\mathbf{B}}_p$  for all  $k (= 1, \dots, M)$ . Thus, the problem is formulated by

$$\min_{\mathbf{F}_d} \|\tilde{\mathbf{A}}_{pd} + \tilde{\mathbf{B}}_p\mathbf{F}_d\| \quad \text{s. t.} \quad \tilde{\mathbf{A}}_{pdM} + \tilde{\mathbf{B}}_{pM}\mathbf{F}_d = \mathbf{O}. \quad (36)$$

The above constraint is the condition that the controller includes the disturbance model, which assures the convergence of  $\mathbf{x}_p[i]$  at the sampling points ( $k = M$ ).

From the Lagrange's undetermined multiplier method, the solution of (36) is obtained by

$$\mathbf{F}_d = \mathbf{Z}[\mathbf{Y}^T(\mathbf{Y}\mathbf{Z}\mathbf{Y}^T)^{-1}\mathbf{Y}\mathbf{Z}\mathbf{X}^T - \mathbf{X}^T, -\mathbf{Y}^T(\mathbf{Y}\mathbf{Z}\mathbf{Y}^T)^{-1}]\tilde{\mathbf{A}}_{pd}, \quad (37)$$

where  $\mathbf{X} := [\tilde{\mathbf{B}}_{p1}^T, \dots, \tilde{\mathbf{B}}_{p(M-1)}^T]^T$ ,  $\mathbf{Y} := \tilde{\mathbf{B}}_{pM}$ ,  $\mathbf{Z} := (\mathbf{X}^T\mathbf{X})^{-1}$ , and the Frobenius norm is adopted in (36).  $M$  should be selected more than  $N$  to assure the non-singularity of  $\mathbf{Z}$ .

## 4 Applications to HDD

In the head-positioning control of hard disk drives, the control strategy is divided into three modes; seeking mode, settling mode, and following mode. In the seeking mode, the head is moved to the desired track as fast as possible. Next, the head is settled to the track without overshoot in the settling mode. After that, the head need to be positioned on the desired track while the information is read or written. In the following mode, the head is positioned finely on the desired track under the vibrations generated by the disk rotation and disturbance.

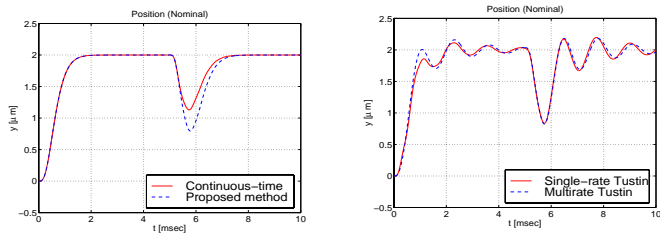
In this section, the proposed feedback controllers are applied to the settling and following modes. While servo signals are detected at a constant period about 100  $[\mu\text{s}]$ , the control input can be changed 2~4 times between one sampling period in the recent hardware [3]. Therefore, the proposed approaches are applicable.

### 4.1 Vibration suppression control based on multirate control

Let the nominal model of this plant be

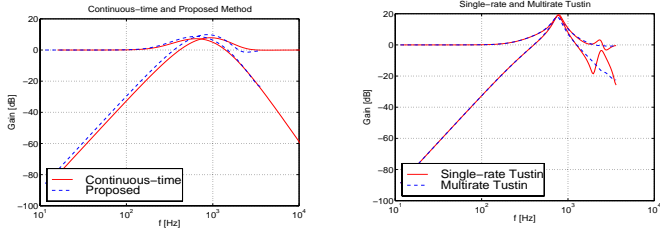
$$P_c(s) = \frac{K}{Ms^2} \frac{\omega_{1n}^2}{s^2 + 2\zeta_{1n}\omega_{1n}s + \omega_{1n}^2}, \quad (38)$$

where  $\omega_{1n} = 2.7 \times 10^3$  [rad/sec] and  $\zeta_{1n} = 0.1$ . This model is obtained from the experimental setup of 3.5-in hard disk drive [3]. The sampling time and input multiplicity of this drive are  $T_y = 138.54$   $[\mu\text{s}]$  and  $N = 4$ .



(a) Proposed controller

(b) Tustin

**Figure 5:** Step and disturbance responses.

(a) Proposed controller

(b) Tustin

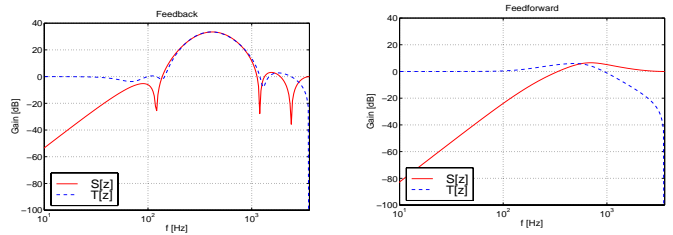
**Figure 6:** Frequency responses  $S[z], T[z]$ .

As shown in Fig. 4(a), the actual plant has the first mechanical resonance mode around 2.7 [kHz], and its variation range is  $\pm 500$  [Hz]. The Nyquist frequency (3.6 [kHz]) is close to this resonance mode. Therefore, it is very difficult to suppress the vibration in the conventional single-rate controller.

Continuous-time controller is designed by regulator and disturbance observer, in which the disturbance is modeled by the step type function  $d(s) = 1/s$ , the poles of the regulator are set to  $(s + \omega_c)^4$ , and those of the observer are set to  $(s + \omega_c)^2(s^2 + 2\zeta_1\omega_{1n}s + \omega_{1n}^2)$ . As shown in Fig. 4(b), this controller has notch characteristic at the resonance frequency. The parameter  $\omega_c$  is tuned so that the bandwidth of the closed-loop system is set as high as possible, and stabilize the  $\pm 1$  [kHz] resonance variation. Fig. 4(b) also shows that the Tustin transformation has large approximation error because the resonance mode is close to the Nyquist frequency.

Simulated results are shown in Fig. 5, which indicates that the proposed method has better performance than the Tustin transformations. In Fig. 5(b), "Multirate Tustin" method is composed of the digital controller discretized by Tustin transformation on  $T_y/N$  and the interpolator which has an up-sampler and a zero-order-hold [11]. While the responses of the Tustin transformations are oscillated, that of the proposed method has no vibration and identical step response with ideal continuous-time system.

Fig. 6 shows the sensitivity and complementary sensitivity functions  $S[z], T[z]$  of the closed loop systems. As shown in Fig. 6(a), the proposed method can remain the ideal characteristics of the original continuous-time controller, because the proposed method is based on the closed-loop system. On the other hand, in the conventional Tustin transformations (Fig. 6(b)), the closed-systems are quite different from the original analog system, because those controllers are discretized based



(a) Feedback

(b) Feedforward

**Figure 7:** Frequency responses  $S[z], T[z]$ .

only on the open-loop characteristics.

## 4.2 Repetitive control based on multirate control

In this section, the proposed multirate repetitive controllers are applied to the following mode. In the following mode, two kinds of disturbance at the output of the plant  $d_y(t)$  should be considered; repeatable and non-repeatable runout. Repeatable runout (RRO) is synchronous with the disk rotation, and non-repeatable runout (NRRO) is not synchronous. In this paper, the RRO is perfectly rejected by the proposed repetitive controllers at  $M$  inter-sample points.

For simplification, the plant is modeled by

$$P_c(s) = \frac{K}{Ms^2}, \quad (39)$$

and RRO are considered at 1st, 10th, and 20th order<sup>1</sup>.

$$d(t) = \sum_{k=1,10,20} a_k \cos k\omega_0 t + b_k \sin k\omega_0 t, \quad (40)$$

where  $\omega_0 = 2\pi 120$  [rad/sec].

Fig. 7 shows the closed-loop characteristics both of the feedback (Fig. 2) and feedforward (Fig. 3) repetitive control systems. Fig. 7(a) indicates the disadvantages of the feedback repetitive controller, where the closed-loop characteristics become worse and difficult to assure stability robustness. On the other hand, in the proposed feedforward repetitive control (Fig. 3), the closed-loop characteristics depends only on  $C_2[z]$  which do not need to have the internal model of (40). Therefore, the feedback characteristics are better than the feedback approach as shown in Fig. 7(b).

Fig. 8 shows the simulated results of the proposed repetitive feedforward control on  $M = N/n$  under the 20th order sinusoidal runout. The switch turns on at just  $t_0 = 10$  [ms]. As shown in Fig. 8(a), the position error converges quickly after the switching action. Moreover, it is shown that the proposed initial value compensation (IVC) can prevent the large overshoot. Fig. 8(b) shows that the inter-sample response of the conventional single-rate controller has large error in the steady state. On the other hand, the errors of the plant position and velocity become zero at every  $T_y/2$  by the

<sup>1</sup>In practice, these modes should be selected by the experimental analysis.

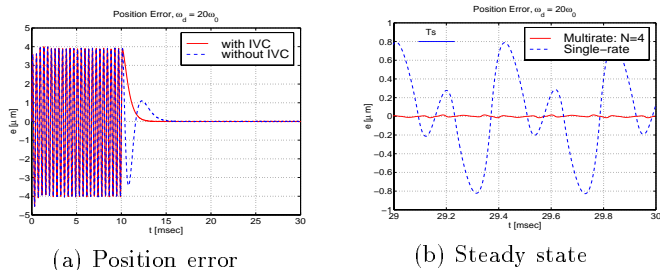


**Figure 8:** Feedforward repetitive control.

$$d_y(t) = T_p \sin k\omega_0 t, T_p = 3.6\mu\text{m}, k = 20.$$

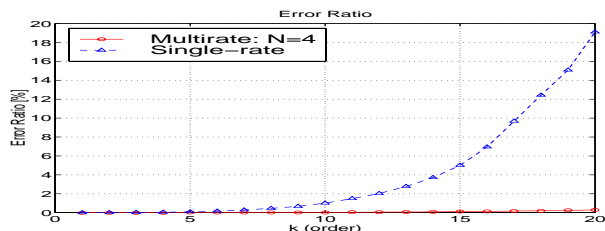


**Figure 9:** Error ratio  $E_R(k)$ .  
(20th order corresponds to 2.4 [kHz].)

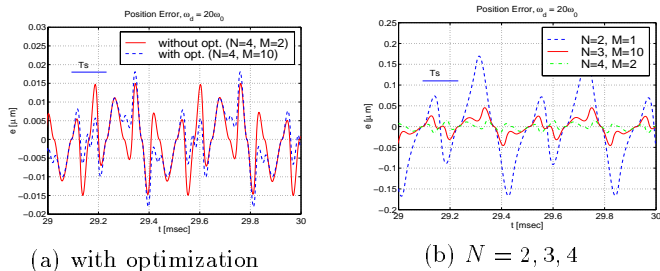


**Figure 10:** Optimized inter-sample response.

proposed controllers<sup>2</sup>. Moreover, the inter-sample position error of the proposed multirate method is much smaller than that of the single-rate controller.

Fig. 9 shows analyzed results of the error ratio  $E_R(k)$  for the disturbance order  $k$ . Considering the inter-sample response, the error ratio is calculated by

$$E_R^2(k) := \frac{\int_{t_s}^{t_s+kT_0} e^2(t) dt}{\int_{t_s}^{t_s+kT_0} d_y^2(t) dt}, \quad (41)$$

where  $d_y(t) = T_p \sin k\omega_0 t$ ,  $T_0 = 2\pi/\omega_0$ , and  $t_s$  is selected as 20[s] in order to evaluate the steady state. In the high frequency region close to the Nyquist frequency (3.6[kHz]), the disturbance rejection performance is much improved by the proposed multirate control, compared with the single-rate controller. Therefore, it is found that the proposed method can demonstrate much effective performance for high-order disturbance.

In the above simulations (Fig. 7 ~ 9), the state multiplicity is selected as  $M = N/n (= 2)$  to reject the disturbance perfectly at  $M$  inter-sample points. In Fig. 10, however, the inter-sample performance is optimized by (37).

<sup>2</sup>In the proposed method, the perfect disturbance rejection is assured  $M (= N/n_p = 4/2 = 2)$  times during  $T_y$ .

As shown in Fig. 10(a), the optimized inter-sample response on  $M = 10$  is not improved so much compared with the case of without the optimization on  $M = 2$ . Therefore, it can be said that the selection of  $M = N/n$  proposed in section 3.1 is valid in engineering sense because  $F_d$  of (31) is simpler than that of (37). However, the optimization approach is valuable because it is applicable to the case that  $N/n$  is non-integer. As shown in Fig. 10(b), the inter-sample performance is improved in higher input multiplicity  $N$ .

## 5 Conclusion

In this paper, the digital control systems which had hardware restrictions of  $T_u < T_y$  were assumed, novel multirate feedback controllers were proposed, which achieved vibration suppression and disturbance rejection in the semi-Nyquist frequency region. Moreover, the inter-sample disturbance rejection performance has been optimized by the fast sampling approach.

Furthermore, the proposed methods were applied to the settling and following modes of the hard disk drive. The advantages of these approaches were demonstrated by the simulations.

Finally, the authors would like to note that part of this research is carried out with a subsidy of the Scientific Research Fund of the Ministry of Education.

## References

- [1] W.-W. Chiang, "Multirate state-space digital controller for sector servo systems," in *Conf. Decision Contr.*, pp. 1902–1907, 1990.
- [2] P. A. Weaver and R. M. Ehrlich, "The use of multirate notch filters in embedded-servo disk drives," in *Amer. Control Conf.*, pp. 4156–4160, June 1995.
- [3] H. Fujimoto, Y. Hori, T. Yamaguchi, and S. Nakagawa, "Proposal of perfect tracking and perfect disturbance rejection control by multirate sampling and applications to hard disk drive control," in *Conf. Decision Contr.*, pp. 5277–5282, 1999.
- [4] H. Fujimoto, A. Kawamura, and M. Tomizuka, "Generalized digital redesign method for linear feedback system based on N-delay control," *IEEE/ASME Trans. Mechatronics*, vol. 4, no. 2, pp. 101–109, 1999.
- [5] S. Hara, Y. Yamamoto, T. Omata, and M. Nakano, "Repetitive control system – a new-type servo system," *IEEE Trans. Automat. Contr.*, vol. 33, pp. 659–668, 1988.
- [6] C. Kempf, W. Messner, M. Tomizuka, and R. Horowitz, "Comparison of four discrete-time repetitive algorithms," *IEEE Contr. Syst. Mag.*, vol. 13, no. 5, pp. 48–54, 1993.
- [7] M. Araki and T. Hagiwara, "Pole assignment by multirate-data output feedback," *Int. J. Control*, vol. 44, no. 6, pp. 1661–1673, 1986.
- [8] T. Chen and B. Francis, *Optimal Sampled-Data Control Systems*. Springer, 1995.
- [9] Y. Yamamoto, A. G. Madievski, and B. D. O. Anderson, "Computation and convergence of frequency response via fast sampling for sampled-data control systems," in *Conf. Decision Contr.*, pp. 2157–2162, 1997.
- [10] T. Chen and L. Qiu, " $H_\infty$  design of general multirate sampled-data control systems," *Automatica*, vol. 30, no. 7, pp. 1139–1152, 1994.
- [11] Y. Gu, M. Tomizuka, and J. Tornero, "Digital redesign of continuous time controller by multirate sampling and high order holds," in *Conf. Decision Contr.*, pp. 3422–3427, 1999.